Solar variability in the past and palaeoclimate data pertaining to the southwest monsoon

Manish Tiwari[1,*] and Rengaswamy Ramesh

Planetary and Geosciences Division, Physical Research Laboratory, Ahmedabad 380 009, India
[1]Present address: National Centre for Antarctic and Ocean Research, Vasco-da-Gama 403 804, India

A significant part of the earth's climate variability is caused by changes in the solar emission. Instrumental observation of the sun gives us some idea about decadal variability in the solar radiation. On longer timescales, we look to palaeoclimate proxies to learn about solar variability. In this review we discuss various palaeo-records and what we have learnt from them. In addition, we outline important questions that need to be addressed.

Keywords: Insolation, palaeoclimate, solar variability, southwest monsoon, total solar irradiation.

THE sun is the sole source of energy for the earth's climatic processes. Any departure from the balance between the energy received from the sun and that radiated back to space is bound to change the climate of the earth[1,2]. The earth's climate is known to exhibit variability at different timescales ranging from annual to millennial. Various causes that govern climatic variability at different timescales have been identified, which can be mainly grouped into internal and external causes. Internal causes involve (i) oscillations in ocean–atmosphere system (e.g. thermohaline circulation changes that re-distribute heat between the tropics and polar regions), (ii) volcanic eruptions (aerosols and other fine particles injected into the atmosphere that prevent solar radiation from reaching the earth surface), (iii) changes in atmospheric concentration of greenhouse gases (such as CO_2, CH_4, NO_2, CFCs, O_3 that absorb the outgoing long-wave radiation), (iv) water vapour and low altitude clouds that form an important feedback mechanism (more the warmth, more the water vapour, which in turn absorbs more of the outgoing radiation), and (v) ice cover and vegetation extent (that control the albedo, i.e. the ratio of the reflected to the incident radiation and act as another feedback mechanism). The external causes include (i) variations in the incoming solar radiation due to changes in the sun–earth geometry (the so-called Milankovitch cycles involving changes in the eccentricity of the earth's orbit, its obliquity and precession of the perihelion; it should be noted that only the change in eccentricity affects the solar energy reaching the earth, while the other two just redistribute heat among different latitudes), and (ii) variation in the incoming solar irradiance at various wavelengths due to changes in the solar activity itself, is thought to affect the earth's climate on decadal to millennial timescales[3,4]. This has gained much credence lately and is the subject of this article. Eddy[5] was the first to suggest that long-term changes in solar activity can affect climate with colder climate during periods of lower solar activity. This was further reinforced by Reid[6], who found a remarkable similarity between the globally averaged sea surface temperature (SST) and the solar activity.

*For correspondence. (e-mail: manish@ncaor.org)

Solar variability

The top of the earth's atmosphere receives solar energy of about 1367 Wm^{-2} and before the dawn of the satellite era it was thought to be a constant (hence known as the 'solar constant') as it was difficult to detect small variations in it due to the presence of the atmosphere. But since 1978, radiometers are being sent into space (satellites). This revealed that the 'solar constant' is not a constant, but varies with an rms amplitude[7] of 0.1%, as shown in Figure 1. Hence a more unique quantity, viz. Total Solar Irradiance (TSI) has been evolved, which is defined as the value of the integrated solar energy flux over the entire electromagnetic spectrum through an area of 1 sq. m oriented towards the sun arriving at the top of the terrestrial atmosphere at the distance of 1 AU (astronomical unit, the mean distance between the sun and the earth[8,9]). Another commonly used term is 'insolation' (Incoming Solar Radiation) that describes the solar energy reaching the earth's surface and depends on the specific latitude, season and angle of incidence. Various processes have been proposed to explain the observed changes in TSI. These include changes in solar diameter[10], transport through the solar convective and radiative zone[11], temperature of the solar photosphere[12], and amount and distribution of magnetic flux on the solar surface[13,14]. The last of these, i.e. perturbation in magnetic flux is assumed to cause TSI variability in most of the recent reconstructions[9].

The magnetic field manifests itself on the solar surface in the form of sunspots and associated active region faculae and bright network[16]. Sunspots are regions with lower temperature than the surrounding regions, and hence appear darker. The relatively colder nature of the sunspots is not

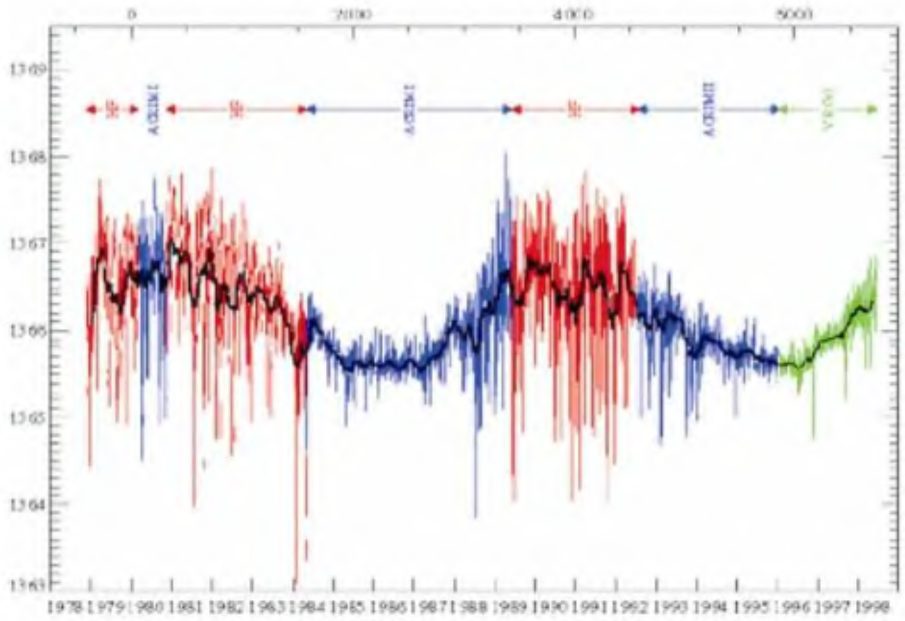

Figure 1. Composite of daily average value of total solar irradiance from different-satellite borne radiometer measurements. HF (Hickey–Frieden cavity radiometer) on NIMBUS 7, ACRIM I and II (Active Cavity Radiometer) on SMM (Solar Maximum Mission) and UARS (Upper Atmosphere Research Satellite) respectively, and VIRGO (Variability of Irradiance and Gravity Oscillation Experiment) on the SOHO (Solar and Heliospheric Observatory). The broad dark line depicts the two-year low-pass filtering[15].

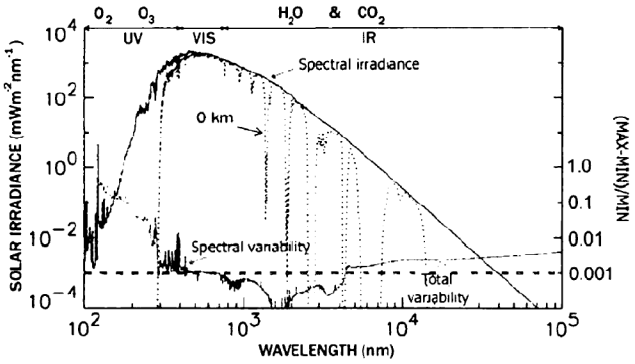

Figure 2. Solar irradiance reaching the top of the atmosphere as a function of wavelength. Dotted line represents irradiance reaching the earth's surface after absorption by ozone in the UV region and by atmospheric gases in the near IR region. Also shown is TSI variability in different spectral bands. The horizontal dashed line depicts variability (right-hand side scale) in the solar irradiance along the 11-year solar cycle[19].

well understood, but it is believed that the strong magnetic field inhibits convection underneath them. The sunspots are confined to 35°N and 35°S solar latitudes. They form in the higher latitudes and migrate towards the solar equator as their size expands (can grow up to ~80,000 km in diameter). The number of sunspots is not constant but varies with a 11-yr 'solar cycle' (also known as Schwabe cycle) that is related to the 22-yr hale cycle of the reversal of the Sun's magnetic field. During higher solar activity, the number of sunspots increases. But the sun, on an average, is brighter during the higher sunspot numbers as brightening due to the faculae and the network outweighs the darkening due to enhanced sunspots[17].

Variability in solar spectrum

The solar flux reaching the top of the earth's atmosphere is composed of many wavelengths that correspond to blackbody radiation at 5770 K, with the maximum radiation falling in the visible and longer wavelengths (Figure 2). Also evident from Figure 2 is that most of the ultraviolet (UV) energy and a considerable portion of the near IR (infrared) is absorbed by ozone and other atmospheric gases. One conspicuous feature is that the TSI variability is mainly limited to wavelengths below 500 nm and is considerably more for shorter wavelengths, i.e. in UV than that observed in the visible region. In the UV region, solar cycle irradiance changes of ~20% near 140 nm, 8% near 200 nm and 3% near 250 nm have been observed[18], whereas TSI variability during a solar cycle is ~0.1%[15,19].

The short wave part of the spectrum (<400 nm) contributes only 7% of the total irradiance[8], but can be an important parameter affecting the climate if there is a mechanism that is exceptionally sensitive to even minor variations in it.

Solar periodicities

The sun is a dynamic star and changes on timescales ranging from minutes to billion of years[8]. The most well-

known cycle is the 11-year solar cycle that was first noted in 1843 by an amateur solar astronomer, H. Schwabe based on the changing number of sunspots. The related cycle is the 22-year Hale cycle (first described by George Hale in early twentieth century), in which the magnetic polarity of the sun reverses and then returns back to the original state. Periodicities longer than this are harder to observe due to limitation of the observational data. However, with the help of proxy records (such as cosmogenic radionuclides, to be discussed later), even longer cycles can be detected. The most important long cycles are the 88-yr Gleissberg cycle and the 208-yr Suess cycle. Proxy records also indicate longer cycles such as ~2300-yr Hallstatt cycle[20]. Based on sunspot numbers and cosmogenic nuclides, several periods of low solar activity have been identified: Oort minimum (AD 980–1120), Wolf minimum (AD 1282–1342), Spörer minimum (AD 1416–1534), Maunder minimum (AD 1645–1715) and Dalton minimum (AD 1790–1820)[8].

Reconstructing past solar irradiance

Direct measurement of TSI is available for the past ~25 years and reconstructed TSI (based on sunspot numbers) is available for only ~300 years. There are various evidences (e.g. based on the study of other sun-like stars) that indicate that the solar activity might exhibit much wider variations than that observed so far. Hence, it becomes necessary to reconstruct the past fluctuations in solar irradiance to fully comprehend the natural variability in TSI on centennial to millennial timescales and to decipher the complete range of inherent periodicities. The best proxies to decipher past TSI variations are the cosmogenic radionuclides (e.g. ^{14}C, ^{10}Be, etc.) as their atmospheric production depends on the cosmic ray flux, which in turn is modulated by solar activity[9]. Cosmic rays are energetic particles originating outside the earth and are mainly composed of protons (~90%), alpha particles, electrons, gamma rays and other atomic nuclei. The net flux of cosmic rays reaching the earth is low, but the energy of individual particles can be very high (averaging several billion electron volts). Hence cosmic rays interact strongly with matter. They produce radionuclides in two ways: by direct bombardment of target atoms or by secondary neutrons. These neutrons are produced by the interaction of cosmic rays with atmospheric molecules and are further slowed to 'thermal energies' by repeated collisions. These slow neutrons are able to effectively interact with stable atoms of the earth's atmosphere[21]. As the cosmic rays approach the earth, they encounter solar wind and the associated magnetic field, which deflects them away from the earth. During higher solar activity, deflection due to the solar magnetic field is more; hence less galactic cosmic rays reach the earth's atmosphere, resulting in lower production of cosmogenic nuclides. Moreover, the earth's magnetic field also deflects away the incoming galactic cosmic rays, which will affect the cosmogenic radionuclides (e.g. the dipolar part of the magnetic field of the earth has decreased by nearly 8% over the last 150 years).

Carbon-14 as solar activity proxy

Radiocarbon (^{14}C) is produced in the atmosphere by the interaction of cosmic ray-produced neutrons with nitrogen nuclei by the (n, p) reaction:

$$^{14}N_7 + {}^{1}n_0 \rightarrow {}^{14}C_6 + {}^{1}H_1$$

This radiocarbon atom is oxidized to $^{14}CO_2$ rapidly and is taken up by the plants and trees during photosynthesis. The ^{14}C decays by β-emission to stable ^{14}N with a half-life of ~5730 years. To reconstruct the past ^{14}C activity, materials such as annual growth rings of trees, annual bands of corals and varve (annual) sediments have been used[22]. Past ^{14}C activity is expressed as $\Delta^{14}C$ that has been corrected for decay corresponding to its age and the fractionation ^{14}C atom experiences while being incorporated. It is expressed in per mil (‰) units with respect to an international standard (NBS oxalic acid).

$$\Delta^{14}C = [(R_{sp}/R_{st}) - 1] \times 10^3‰,$$

where R_{st} is $^{14}C/^{12}C$ ratio or activity in the standard. R_{sp} is $^{14}C/^{12}C$ ratio or activity in the sample and given as:

$$R_{sp} = R_{ms}\,[1 - \{2(25 + \delta^{13}C)/1000\}],$$

where R_{ms} is the measured $^{14}C/^{12}C$ ratio or activity.

$\delta^{13}C$ is the deviation in the $^{13}C/^{12}C$ ratio of the sample with respect to a suitable international standard[23] (e.g. V-PDB, in the case of carbonates) expressed in ‰ (for experimental procedures see Yadava and Ramesh[24]).

Apart from the solar wind and the associated magnetic field effect, another factor affecting ^{14}C production is the earth's magnetic field, as it deflects away the incoming galactic cosmic rays. Studies have found that there is a long-term change in ^{14}C production due to the changing geomagnetic field intensity, which has been approximated and the corrected ^{14}C activity obtained is called the 'residual $\Delta^{14}C$ value'[25]. The $\Delta^{14}C$ values thus reconstructed have been shown to exhibit good correlation with the available sunspot record (considering the fact that the two are entirely different observations) with lower ^{14}C activity during higher sunspot numbers, i.e. enhanced solar activity[25] (Figure 3).

It is clearly indicated that $\Delta^{14}C$ can act as a good proxy for the past solar activity and reliable records extending back to ~35,000 years BP have been constructed[26–28]. Recently, attempts have been made to reconstruct solar

activity changes for the past 32,000 years using cosmogenic *in situ* ^{14}C in ice of Greenland[29]. The advantage is that at such high latitudes, the effect of geomagnetic field fluctuation is negligible. More importantly, climatic variations which affect the distribution of ^{14}C between different reservoirs (such as atmosphere, surface and deep-ocean, etc.) are insignificant as in the case of polar ice the ^{14}C is produced *in situ* by nuclear interactions of fast neutrons with oxygen nuclei. In contrast, ^{14}C produced in the atmosphere is distributed between various reservoirs such as the biosphere, mixed layer of the ocean and the deep ocean. If the production of deep-ocean water reduces, then the concentration of ^{14}C in the atmosphere will increase. For example, during the last glacial period, the atmospheric $\Delta^{14}C$ increased by 100‰ due to reduced oceanic (thermohaline) circulation[30].

Beryllium-10 as solar activity proxy

The radioactive nuclide, ^{10}Be is produced in the atmosphere due to cosmic ray induced spallation of nitrogen and oxygen atoms. ^{10}Be can also be produced in the exposed rocks and soil by *in situ* production. It decays[31] by β-emission to ^{10}B with a half-life of 1.51 Myr. ^{10}Be sticks to aerosols and is scavenged by precipitation. Consequently, the residence time of ^{10}Be is short (1 week to 2 years) that prevents its homogenization in the atmosphere and is deposited at the latitude at which it is produced. In the polar regions, atmospheric ^{10}Be is deposited in the ice and snow directly and is used as a proxy for solar activity. Beer *et al.*[32] have made a comparison between the ^{10}Be record from the Greenland ice sheet and the northern hemisphere temperature record and found good correlation: during periods of lower ^{10}Be concentration, i.e. higher solar activity, the temperatures were higher (Figure 4).

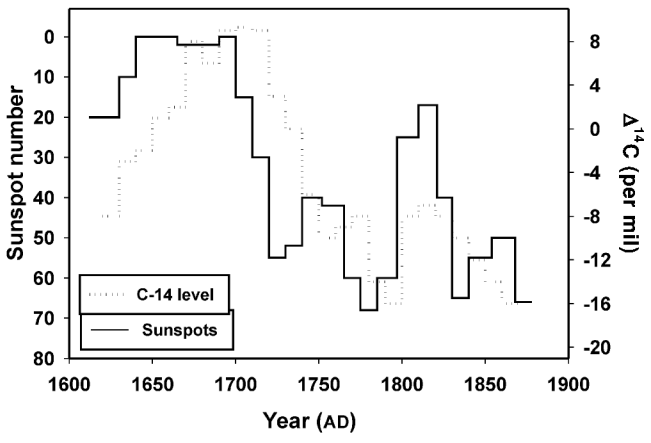

Figure 3. Comparison between $\Delta^{14}C$ record (obtained from tree rings) and sunspot numbers (average of sunspot numbers over each 11-yr solar cycle). Note that the sunspot number axis is reversed with values increasing downwards[25].

The concentration of ^{10}Be in marine sediments depends not only on the cosmic ray flux but also on the (sedimentation) rate at which ^{10}Be atoms are removed from the sea surface to the bottom sediments. In spite of this limitation, a globally stacked record of ^{10}Be concentration from marine sediments has been reconstructed, that yields relative variations in ^{10}Be production rate for the past 200,000 years[33]. Based on this record, Sharma[34] has shown that solar activity exhibits a cycle of 100,000-years that is strongly correlated to the 100 ka glacial–interglacial cycle, and proposed that solar activity controls the climatic variations on a 100,000 yr timescale.

Effect of solar variability on terrestrial systems

Solar variability in different spectral bands affects the various interlinked systems operating on earth. Though the total observed TSI variations[19] using the satellite-borne radiometer is 0.1%, it has been estimated (using the study of sun-like stars) that TSI might be lower by 0.25% during the Maunder minimum (AD 1645–1715) than at present[37,38]. Lean *et al.*[37] further proposed that a decrease of 0.25% in TSI might lower the global equilibrium temperature by 0.2–0.6°C. Even a decline of 0.15% in TSI might affect the earth's climate by various feedback processes as different spectral bands (e.g. UV region) constituting the TSI interact differently with terrestrial systems. Mainly, three different mechanisms have been invoked involving the indirect effect of TSI variations on the earth's atmosphere. The first involves the heating of the earth's stratosphere by increased absorption of solar UV radiation by ozone during periods of enhanced solar activity[39,40]. Solar irradiance varies much more in the UV spectral band (up to 20%) during a solar cycle compared to the TSI (~0.1%). The positive feedback is that more the UV, more the ozone production and more the heating. This heating is transferred to the troposphere as shown by the theoretical models[40]. It further affects atmospheric circulation, e.g. increased tropospheric Hadley circulation

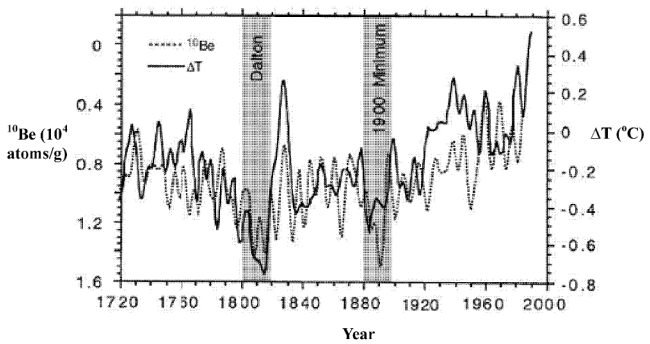

Figure 4. Comparison between the northern hemisphere temperature record[35,36] and ^{10}Be concentration in Dye 3 ice core from Greenland[32]. Note that ^{10}Be concentration scale is reversed.

reported during enhanced solar activity[41] affects the distribution of atmospheric moisture.

The second mechanism is that during periods of higher solar activity, the flux of galactic cosmic rays to the earth is reduced, generating less cloud condensation nuclei, and resulting in less cloudiness[40]. Friis-Christensen and Svensmark[42] have reported good correlation between the 12 months running means of the total cloud cover (data obtained from the International Satellite Cloud Climatology Project) and cosmic ray intensity measured at Climax Neutron Monitor Station, Colorado, which comes out to be 0.93. Reduction in cloud cover is significant [a decrease of 3% from 1987 (solar minimum) to ~1990 (increasing solar activity)], which would result in global warming[43] corresponding to 1–1.5 Wm^{-2}.

An alternative mechanism has been proposed that involves coupling between the ionosphere and troposphere[44]. Ionosphere is the region in the atmosphere (at the altitude of ~80–250 km) where the atoms absorb the incoming solar energy in the UV band and produce ions and free electrons. The varying solar activity also varies with the ionospheric charge, which is intimately coupled with tropospheric thunderstorms. Variations in ionospheric electric field will thus affect the electric charge on the clouds, which in turn plays an important role in coalescence of droplets and condensation of water vapour[45].

Another positive feedback occurs in the way that more the condensation, more will be the latent heat release that will further heat up the troposphere and cause enhanced evaporation.

Sun–monsoon connection

Attempts to correlate solar irradiance with monsoon rainfall revealed no consistent relationship at the 11-yr timescale[46]. On the other hand, the relation between instrumental records of the Indian monsoon rainfall and sunspot activity was investigated by Hiremath and Mandi[47], who concluded that (i) the southwest (SW) monsoon rainfall variabilities had significant positive correlations with the sunspot activity during 1871–2000, and (ii) FFT and wavelet analyses of the SW monsoon rainfall variability show the periods 2.7, 16 and 22 yrs respectively, which are similar to the periods found in sunspot occurrence data. Recently, Bhattacharya and Narasimha[48] have studied the available meteorological Indian rainfall data with four solar variability indices and reported that both are highly correlated at decadal to bi-decadal timescales. There have been various palaeoclimatic studies as well, indicating that the sun plays a major role in governing the variations as observed in the Asian monsoon on decadal to millennial timescales. For example, Neff *et al.*[49] studied speleothem samples from Oman for the period 9–6 ka and compared them with the $\Delta^{14}C$ record from tree rings, which is dependent on cosmic ray fluxes modulated by solar activity. They found good correlation between the monsoon and solar activity proxies and suggested that variation in solar radiation exhibits a prominent control over the monsoon system on centennial to decadal timescales. Similarly, Fleitmann *et al.*[50] analysed Holocene stalagmites from Oman and compared $\delta^{18}O$ data with GRIP ice core $\delta^{18}O$ and ^{14}C record from tree rings. They proposed that early Holocene monsoon circulation was controlled by glacial boundary conditions such as northward heat transport in the Atlantic and the thermohaline circulation. After 8 ka, as the thermohaline circulation stabilized, the monsoon circulation responded more directly to solar forcing. One major limitation in the above two studies is that Oman is a desert region and does not receive much monsoon precipitation. Agnihotri *et al.*[51] obtained a core from the eastern Arabian Sea off the Gujarat coast (2502G) and analysed it for three palaeoclimatic proxies (organic carbon, nitrogen and aluminum content of marine sediments) for the past 1200 years and compared it with TSI records (Figure 5). They found nearly similar trends for these proxies and TSI variations. Lower TSI was accompanied by lower productivity, indicating weakened SW monsoon. Spectral analyses of the TSI, palaeoclimatic proxies and Indian summer monsoon rainfall yielded similar periodicities, which led them to propose that solar forcing controls the monsoonal precipitation on multi-decadal timescales. Sarkar *et al.*[52] have analysed oxygen isotope ratios (viz. $\delta^{18}O$) of planktonic foraminifera (*Globigerinoides sacculifer* and *Globorotalia menardii*) in the same core (2502G) as shown in Figure 5 (last panel). Precipitation alters the sea surface salinity in the way that $\delta^{18}O$ of foraminifera decreases with increasing precipitation (discussed in detail in the next section).

As evident from Figure 5, the productivity proxies (viz. C_{org} and N content) governed by the SW monsoon wind strength exhibit good matching with the TSI variations. However, the correlation is lost when the SW monsoon precipitation (run-off) proxies (viz. $\delta^{18}O$ and Al content) are compared with the TSI. Recently Wang *et al.*[53] have carried out high-resolution oxygen isotope analysis (at 5-yr intervals) on a stalagmite from southern China and found that solar variability played a significant role in governing the Asian monsoon at decadal to centennial timescale, similar to the earlier conclusion based on varve sediments off the Karachi coast[54]. Control of solar irradiance on the millennial scale changes in monsoon has been reported by Higginson *et al.*[55], after studying marine sediment cores from the Oman and Pakistan margins, which reinforces earlier study by Staubwasser *et al.*[56]. Ji *et al.*[57] have studied iron oxide content in a sediment core from a lake on the Tibetan Plateau, Central Asia. They found a periodicity of 200 years corresponding to the Suess solar cycle. Table 1 summarizes the results on palaeomonsoon–sun connection.

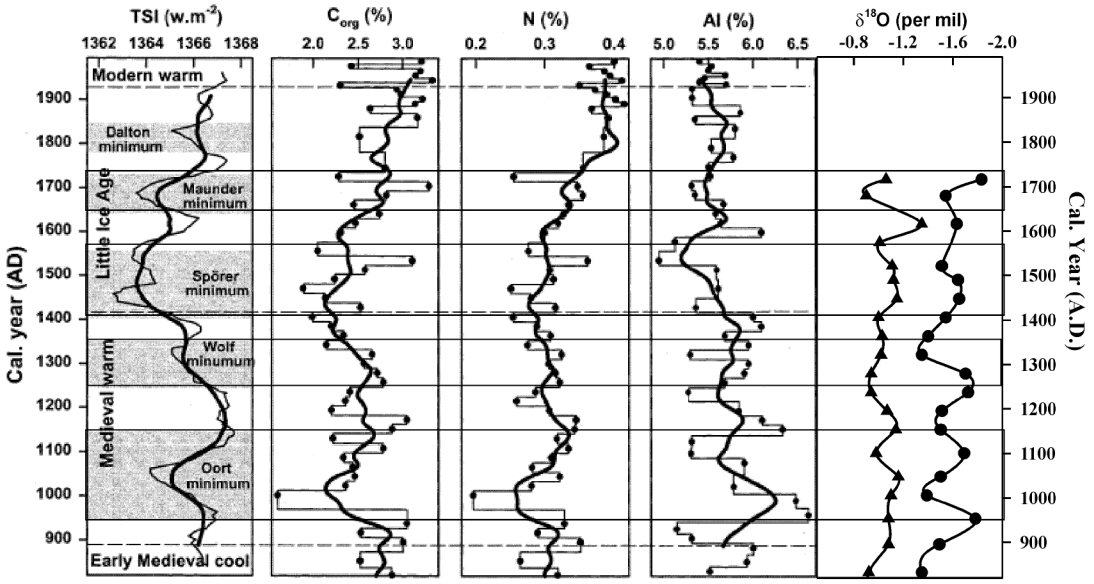

Figure 5. TSI vs C_{org}, N, Al (Agnihotri *et al.*[51]) and $\delta^{18}O$ of planktonic foraminifera *Globigerinoides sacculifer* (depicted by circle, last panel) and *Globorotalia menardii* (depicted by triangle, last panel; data from Sarkar *et al.*[52]).

Table 1. Details of earlier palaeoclimatic studies regarding sun–monsoon connection

Reference	Proxies, materials and study area	Span (yrs BP)	Average resolution	Solar periodicities (yrs)
Castagnoli *et al.*[58]	$CaCO_3$ in core from Ionian Sea	0 to ~1820	~3.87 yrs per sample	~200
Von Rad *et al.*[54]	Thickness of varve sediments off the Karachi coast	0 to ~5000	~7 yrs per sample	~250, 125, 95, 56, 45, 39, 29–31, 14
Hong *et al.*[59]	$\delta^{18}O$ in peat cellulose, NE China	0 to ~6000	~20 yrs per sample	*86, 93, 101, 110, 127, 132, 140, 155, 207, 245, 311, 590, 820, 1046
Hong *et al.*[60]	$\delta^{13}C$ in peat cellulose, NE China	0 to ~6000	~20 yrs per sample	*70, 80, 90, 107, 110, 123, 134, 141, 162, 198, 205, 249, 278, 324, 389, 467, 584, 834, 1060
Neff *et al.*[49]	$\delta^{18}O$ of stalagmite, Oman	~ 6100 to 9600	~4.1 yrs per sample	~1018, 226, 28, 10.7, 9
Agnihotri *et al.*[51]	Organic carbon, N and Al content in a sediment core off Gujarat coast	0 to ~1200	~20 yrs per sample	~200, 105, 60
Leuschner and Sirocko[61]	Wind and upwelling indices in a sediment core, Oman margin	~5000 to 135,000	150–500 yrs per sample	1100, 1450, 1750, 2300
Fleitmann *et al.*[50]	$\delta^{18}O$ of stalagmite, Oman	~400 to 10,300	~4.5 yrs per sample	~220, 140, 90, 18, 11
Staubwasser *et al.*[56]	$\delta^{18}O$ of *Globigerinoides ruber* in a marine sediment core off Pakistan	0 to ~10,000	~17 yrs per sample	~220
Wang *et al.*[53]	$\delta^{18}O$ of stalagmite, Southern China	0 to ~9000	~5 yrs per sample	~512, 206, 148, 24, 22–17, 15–16
Ji *et al.*[57]	Iron oxide content in a lacustrine core, Tibet	0 to ~17,500	~38 yrs per sample	~293, 200, 163, 123
Tiwari *et al.*[62]	$\delta^{18}O$ of three planktonic foraminiferal species in a sediment core off Mangalore coast, India	~450 to 1200	~50 yrs per sample	~200
Gupta *et al.*[63]	Percentage *G. bulloides* in sediment core off Oman Margin	~0 to 11,000	~30 yrs per sample	~1550, 152, 137, 114, 101, 89, 93, 79

*Significance level not specified, many of these peaks could be spurious.

An example from eastern Arabian Sea

The major limitation of these studies was that none of them was from southwestern India (the Western Ghats), the most suitable region for studying past fluctuations in South Asian monsoon, as it receives abundant precipitation during the SW monsoon months (up to 4000 mm/yr)[52]. Moreover, many of these studies relied on the SW monsoon wind strength reconstruction (e.g. those employing productivity records) and not the actual precipitation. To fill this lacuna, we have strategically chosen a sediment core SK145-9 from the eastern Arabian Sea off the Manglore coast (Figure 5, 12.6°N, 74.3°E; water depth = 400 m; dated length = 252 cm)[62]. For this core, we obtained 11 radiocarbon dates spanning ~13,000 calendar years (spanning 252 cm length) providing an average sedimentation rate of 19 cm/10^3 years, with an average resolution of ~50 yr/cm. The top 50 cm has been sampled at every centimetre and below 50 cm sampling was done at every 2 cm. The top 50 cm of this core (sampled closely), covering a time span of approximately 2800 years, has been taken for further studies. Thus it offers high time resolution and therefore will aid in understanding sub-centennial scale variability[62].

All along the Western Ghats (that lies parallel to the western Indian coast from ~20 to ~10°N lat.), intense orographic precipitation takes place that gets into the coastal Arabian Sea as surface run-off and reduces the sea surface salinity considerably. Along the southwestern Indian coast, salinity distribution becomes north-south (Figure 6), with low salinities of up to 34 PSU pointing towards the freshwater influx, and away from the coast salinity rapidly increases[64], reaching up to 36 PSU.

This reduction in salinity is recorded by the oxygen isotopes of water that get incorporated in the calcitic shells of the foraminifera. For oxygen isotope analyses, 30–35 shells of the three species of planktonic foraminifera, viz. *Globigerinoides ruber*, *Gs. sacculifer*, *Gr. menardii* were handpicked and analysed using GEO 20-20 mass spectrometer (Europa Scientific, UK). The external precision on $\delta^{18}O$ measurement was better than ±0.1‰ (1σ standard deviation), as determined by the three daily measurements of an internal calcitic standard (standard error is 0.02‰). All isotopic values were reported with respect to V-PDB. Further experimental details can be found elsewhere[65]. *Gs. ruber* and *Gs. sacculifer* are surface-dwelling species predominantly inhabiting the top 25 and 50 m respectively whereas *Gr. menardii* is a deeper dwelling species[66,67] predominantly inhabiting 100–150 m. Thus an oxygen isotope signal arising due to any surface processes (e.g. salinity change) will be most pronounced in the surface dwelling species, viz. *Gs. ruber* and *Gs. sacculifer* and will be subdued in the deeper dwelling species, i.e. *Gr. menardii*. The factors controlling the oxygen isotopes in foraminiferal shells are the sea surface salinity and sea surface temperature (SST)[68,69]. For the past ~3 ka there has been no salinity fluctuations due to the global ice-volume effect, as there were no significant global ice-melting episodes affecting the sea level[70]. Moreover, SST variations in the tropics for the past 10 ka are small[71] (~0.5°C). The studied species are known to grow predominantly during the SW monsoon months and hence are likely to record signals arising mainly due to SW monsoon fluctuation[72]. In the eastern Arabian Sea, sea surface salinity variation is mainly controlled by the variation in the supply of freshwater as surface run-off from the adjacent Western Ghats during the SW monsoon. With the onset of SW monsoon winds, the upwelling intensifies but as it is mainly controlled by basin-wide remote processes in the Arabian Sea and Bay of Bengal[73,74], variation in the local upwelling intensity will affect the interannual SST changes in a small way[75]. These remote processes are the winds in the Bay of Bengal and the equatorial Indian Ocean that force the upwelling in the eastern Arabian Sea through the propagation of Kelvin waves along the west coast of India[74]. We therefore assume that the dominant factor controlling the $\delta^{18}O$ signals in the eastern Arabian Sea is the sea surface salinity changes induced by the variation in the SW monsoon precipitation. A reduction in sea surface salinity occurs due to the influx of large amount of freshwater, depleted in ^{18}O, as surface run-off into the coastal eastern Arabian Sea during intense SW monsoon precipitation events. In the eastern Arabian Sea, for every per mil decline in salinity, the $\delta^{18}O$ value decreases[76] by 0.33‰. Thus a depleted ^{18}O signal indicates enhanced SW monsoon precipitation, whereas an enriched ^{18}O signal points towards reduced precipitation due to weaker SW monsoon.

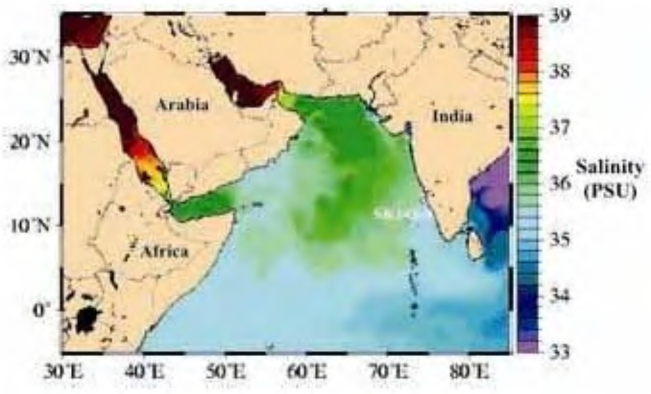

Figure 6. Location of core SK145-9 along with salinity pattern (in PSU) during the SW monsoon months. Salinity rapidly increases away from the southwest coast of India (from Naval Research Laboratory, United States Navy website: www7320.nrlssc.navy.mil/global_ncom/ara.html).

The solar connection

Bard *et al.*[77] reconstructed TSI data for the past 1200 years, which has been used for the present study. They

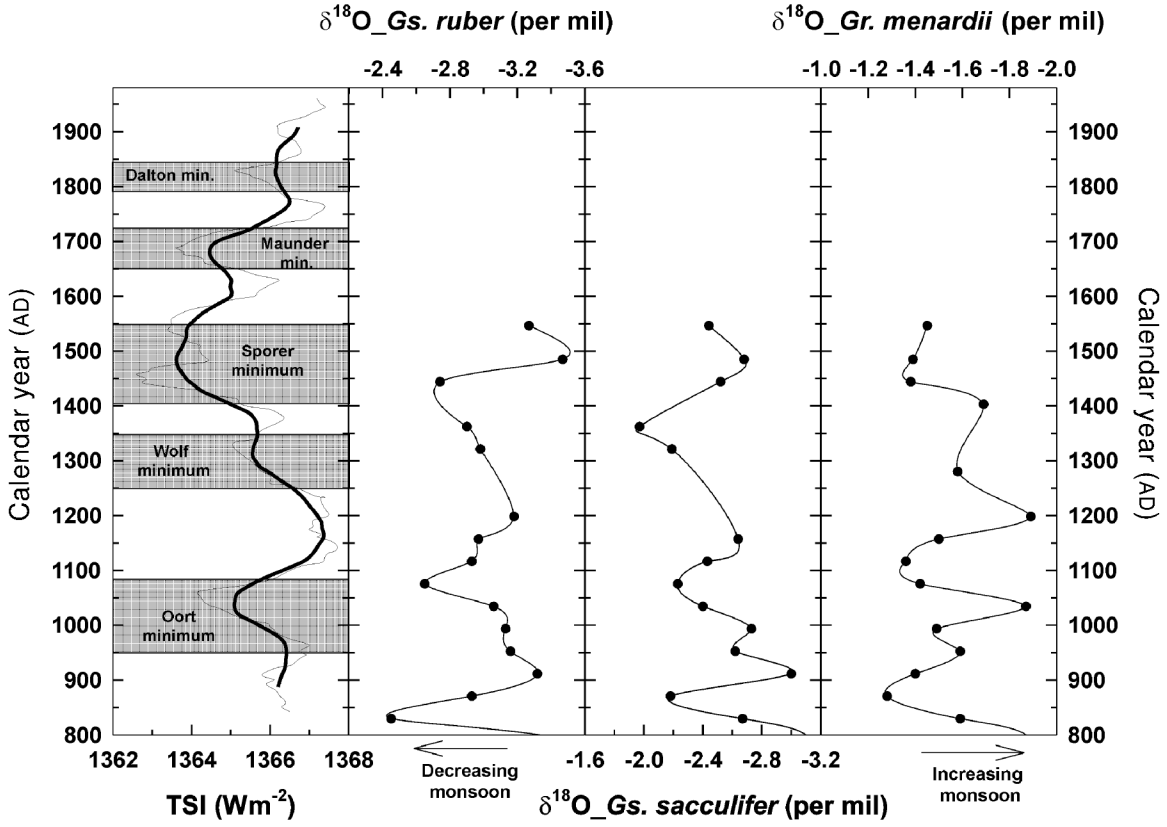

Figure 7. Comparison between TSI (thick line in the first panel depicts ten-point running average) and $\delta^{18}O$ record from the core SK145-9 (Tiwari *et al.*[62]).

based the TSI estimation on the common fluctuations of the ^{14}C and ^{10}Be production rates obtained from tree rings and polar ice sheets. The TSI curve used in this study assumes a 0.25% reduction in TSI during the Maunder minimum[38]. The TSI data are unequally spaced at 8–10 years interval, which is first splined for every 10-years and then a ten point running average is taken so that the resolution of TSI data becomes comparable to that of SK 145-9. Figure 7 shows a comparison between the TSI record and $\delta^{18}O$ in all the three foraminiferal species.

The core SK 145-9 does not extend beyond AD 1550 and TSI data available from AD 850 onwards only; hence comparison can be made for only seven centuries. As evident from Figure 7, precipitation signals from all the three species match reasonably well with TSI fluctuations within the radiocarbon age uncertainties (~80 years). Exact matching is not seen between the precipitation and TSI signals, which could be due to the coarser resolution of the sedimentary record compared to that of the TSI. In general, during periods of lower TSI values, we get lower precipitation, implying solar forcing on the SW monsoon–precipitation on centennial timescale. During periods of reduced solar irradiance, viz. Oort, Wolf and Spörer minima, precipitation also reduces as indicated by enhanced $\delta^{18}O$ values.

To further explore the sun–monsoon connection, spectral analysis was performed that can possibly help in delineating the factors forcing the monsoon. Figure 8 shows the results of spectral analysis on the oxygen isotope time series of the two species of foraminifera for the past ~2900 years using the REDFIT 3.6 program[78]. The $\delta^{18}O$ in *Gr. menardii* exhibits a significant periodicity of ~215 yrs and in *Gs. ruber* it shows a periodicity of ~230 yrs that is just below the 95% significance level. This implies that the SW monsoon follows a dominant quasi-periodicity of ~200 yrs, which is similar to that of the 200-yr Suess solar cycle[79]. In the case of *Gs. sacculifer*, all the frequencies are suppressed and well below the 95% significance level (not shown). *Gs. sacculifer* responds differently, possibly because of its vertical migration in the water column.

Earlier, ~200, 113, ~77 and ~53 yr periodicities have been observed in the TSI data obtained from sunspot numbers and cosmogenic isotopes[51]. Furthermore, power spectra of various proxies controlled by monsoon strength in a core raised from the northeastern Arabian Sea[51] showed significant periodicities of ~200, ~110 and 56 yrs. A recent high-resolution study on a 9000 yr-long speleothem from southern China has revealed prominent periodicities of 558, 206, 159, 24, 22–17, 16–15 yrs in Asian

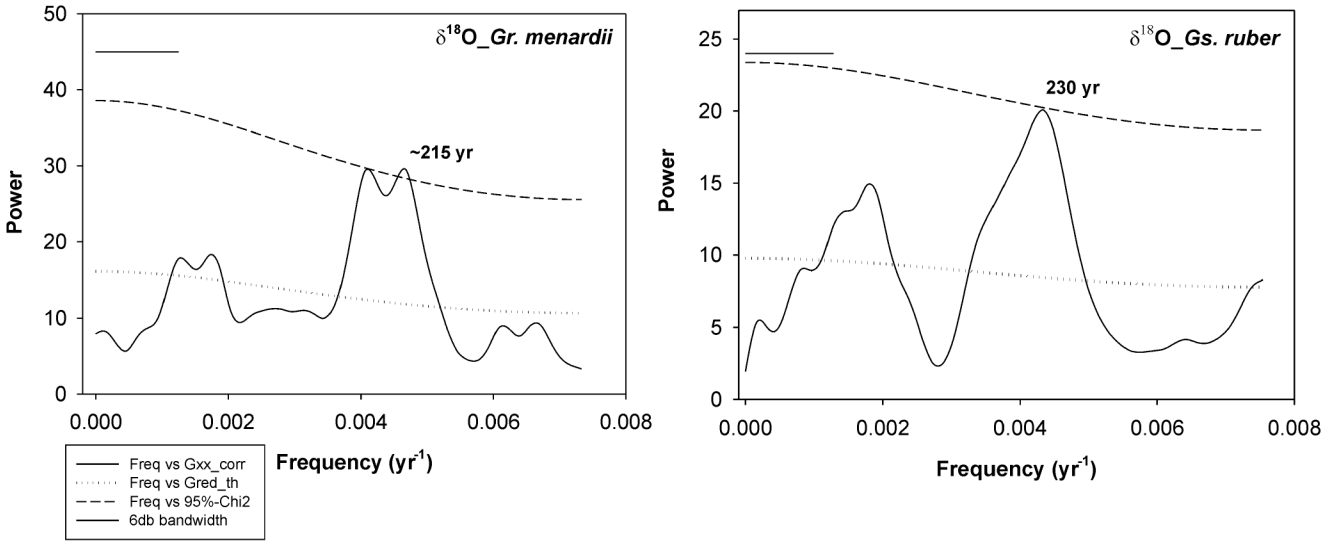

Figure 8. Power spectra of oxygen isotope time series of two species of foraminifera. Horizontal line (upper left-hand corner) represents 6 db bandwidth of the spectral resolution. Gxx_corr denotes amplitude or power of various frequencies. Gred_th (shown by dotted line) is the background signal. Dashed line denotes the 95% significance level calculated using the chi square test.

monsoon[53]. A 200-yr periodicity has also been reported by Ji *et al.*[57] in a sediment core from a Tibetan lake. Most of these periodicities match with those obtained on $\Delta^{14}C$ (controlled by the solar activity), which reinforces the hypothesis that the intensity of the Asian monsoon is affected by variations in solar activity. Lower frequencies are not observed in our study due to the average sample resolution, which is ~65 yrs.

Visual correlation between the TSI and the SW monsoon precipitation along with the periodicities observed in oxygen isotope time series indicates that the SW monsoon intensity is indeed governed by variations in TSI on centennial timescale.

Conclusion

Solar variability influences the climate of the earth, but to varying degrees. Climate models have shown that variations in TSI can explain the pre-industrial increase in temperature (i.e. 0.3°C surface warming from 1650 to 1790), but it accounts for only 0.25°C of the 0.6°C warming experienced from 1900 to 1990[9,80]. It signifies that other forcings (most probably anthropogenic emission of greenhouse gases) are responsible for the rapid increase in surface temperature observed during the 20th century. As far as monsoonal circulation (which forms a major part of the global climate) is concerned, solar variability seems to play a significant role in governing it on decadal to centennial timescales through direct and indirect radiative forcing by enhancing the land–sea temperature contrast.

Despite such advances, several questions remain unanswered. The foremost is to understand the total solar variability on different timescales: what is the total amplitude of TSI variation on a long term and is it sufficient to explain the climatic changes? For this, more accurate and precise reconstruction of the past variations in cosmogenic nuclide concentrations has to be carried out. How do different spectral bands of the TSI behave with varying solar activity? One area that needs urgent attention is the various internal amplification mechanisms, which might significantly alter the climate, even when total variability in TSI is not much. Moreover, the effect of other forcing mechanisms (e.g. thermohaline circulation changes, volcanic and greenhouse gas forcing, albedo changes) has to be clearly delineated. Much work remains to be done to elucidate the relationship between sun and monsoon circulation, which forms a significant part of the global climate. In future, emphasis should be on relating the variability of the specific palaeoclimate data used to a particular part of the solar spectrum. Although various studies have pointed towards decadal to multidecadal scale correlations, centennial to millennial scale correlations still remain to be fully explored. Further, the exact linking mechanism is yet to be found and poses a challenge to the scientific community.

1. Friis-Christensen, E. and Lassen, K., Length of the solar cycle: An indicator of solar activity closely associated with climate. *Science*, 1991, **192**, 1189–1202.
2. Bond, G. *et al.*, Persistent solar influence on North Atlantic climate during the Holocene. *Science*, 2001, **294**, 2130–2136.
3. Mende, W. and Stellmacher, R., Effect of the Earth orbit and solar variability on climate. In *Climate of the 21st Century: Changes and Risks* (eds Lozan, J. L., Graßl, H. and Hupfer, P.), Wissenschaf flische, Hamburg, Germany, 2001, pp. 27–33.
4. Rind, D., The sun's role in climate variations. *Science*, 2002, **296**, 673–677.

5. Eddy, J. A., The Maunder minimum. *Science*, 1976, **192**, 1189–1202.
6. Reid, G. C., Influence of solar variability on global sea surface temperatures. *Nature*, 1987, **329**, 142–143.
7. Foukal, P., Can slow variation in solar luminosity provide missing link between the sun and climate? *EOS*, 2003, **84**, 205–208.
8. Beer, J., Mende, W. and Stellmacher, R., The role of the sun in climate forcing. *Quat. Sci. Rev.*, 2000, **19**, 403–415.
9. Mendoza, B., Total solar irradiance and climate. *Adv. Space Res.*, 2005, **35**, 882–890.
10. Sofia, S. and Fox, P., Solar variability and climate. *Climate Change*, 1994, **27**, 249–257.
11. Hoyt, D. V. and Schatten, K. H., A discussion of plausible solar irradiance variations, 1700–1992. *J. Geophys. Res.*, 1993, **98**, 18895–18906.
12. Kuhn, J. R. and Libbrecht, K. G., Nonfacular solar luminosity variation. *Astrophys. J. Lett.*, 1991, **381**, L35–L37.
13. Foukal, P. and Lean, J., Magnetic modulation of solar luminosity by photospheric activity. *Astrophys. J.*, 1988, **328**, 347–357.
14. Lean, J., Cook, J., Marquette, W. and Johannesson, A., Magnetic sources of the solar irradiance cycle. *Astrophys. J.*, 1998, **492**, 390–401.
15. Fröhlich, C. and Lean, J., The sun's total irradiance: Cycles, trends and climate change uncertainties since 1976. *Geophys. Res. Lett.*, 1998, **25**, 4377–4380.
16. Solanki, S. K., Small scale solar magnetic fields – An overview. *Space Sci. Rev.*, 1993, **63**, 1–188.
17. Solanki, S. K. and Fligge, M., How much of the solar irradiance variations is caused by the magnetic field at the solar surface. *Adv. Space Res.*, 2002, **29**, 1933–1940.
18. Lean, J., Rottman, G. J., Kyle, H. L., Woods, T. N., Hickey, J. R. and Puga, L. C., Detection and parameterization of variations in solar-mid-and-near-ultraviolet radiation (200–400 nm). *J. Geophys. Res.*, 1997, **102**, 29939–29956.
19. Lean, J., Short-term direct indices of solar variability. *Adv. Space Res.*, 2000, **94**, 39–51.
20. Mayewski, P. A., Meeker, L. D., Twickler, M. S., Whitlow, S., Yang, Q., Lyons, W. B. and Prentice, M., Major features and forcing of high-latitude northern hemisphere atmospheric circulation using a 110,000 year-long glaciochemical series. *J. Geophys. Res.*, 1997, **102**, 26345–26366.
21. Dickin, A. P., Cosmogenic nuclides. In *Radiogenic Isotope Geology*, Cambridge University Press, Cambridge, 1997, pp. 360–396.
22. Chakraborty, S., Ramesh, R. and Krishnaswami, S., Air–sea exchange of CO_2 in the Gulf of Kutch, northern Arabian Sea based on bomb-carbon in corals and tree rings. *Proc. Indian Acad. Sci. (Earth Planet. Sci.)*, 1994, **103**, 329–340.
23. Hoefs, J., Theoretical and experimental principles. In *Stable Isotope Geochemistry*, Springer-Verlag, 1997, 4th edn, p. 22.
24. Yadava, M. G. and Ramesh, R., Speleothems – Useful proxies for past monsoon rainfall. *J. Sci. Ind. Res.*, 1999, **58**, 339–348.
25. Stuiver, M. and Quay, P. D., Changes in atmospheric carbon-14 attributed to a variable sun. *Science*, 1980, **207**, 11–19.
26. Stuiver, M. and Braziunas, T. F., Atmospheric ^{14}C and century scale solar oscillations. *Nature*, 1989, **338**, 405–408.
27. Stuiver, M. *et al.*, INTCAL98 Radiocarbon age calibration, 24,000-0 cal BP. *Radiocarbon*, 1998, **40**, 1041–1083.
28. Hughen, K., Lehman, S., Southon, J., Overpeck, J., Marchal, O., Herring, C. and Turnbul, J., ^{14}C Activity and global carbon cycle changes over the past 50,000 years. *Science*, 2004, **303**, 202–207.
29. Lal, D., Jull, A. J. T., Pollard, D. and Vachera, L., Evidence for large century time-scale changes in solar activity in the past 32 kyr, based on *in situ* cosmogenic ^{14}C in ice at Summit, Greenland. *Earth Planet. Sci. Lett.*, 2005, **234**, 335–349.
30. Bard, E., Geochemical and geophysical implications of the radiocarbon calibration. *Geochim. Cosmochim. Acta*, 1998, **62**, 2025–2038.
31. Hoffman, H. J. *et al.*, ^{10}Be half-life and AMS-standards. *Nucl. Instrum. Methods Phys. Res. B*, 1987, **29**, 32–36.
32. Beer, J. *et al.*, Solar variability traced by cosmogenic isotopes. In *The Sun as a Variable Star: Solar and Stellar Irradiance Variations* (eds Pap, J. M. *et al.*), Cambridge University Press, Cambridge, 1994, pp. 291–300.
33. Frank, M., Schwarz, B., Baumann, S., Kubik, P. W., Suter, M. and Mangini, A., A 200 kyr record of cosmogenic radionuclide production rate and geomagnetic field intensity from Be-10 in globally stacked deep-sea sediments. *Earth Planet. Sci. Lett.*, 1997, **149**, 121–129.
34. Sharma, M., Variations in solar magnetic activity during the last 200000 years: Is there a Sun–climate connection? *Earth Planet. Sci. Lett.*, 2002, **199**, 459–472.
35. Groveman, B. S. and Landsberg, H. E., Reconstruction of northern hemisphere temperature: 1579–1880. University of Maryland, College Park, MD, 1979, pp. 79–181.
36. Jones, P. D., Raper, S. C. B., Bradley, R. S., Diaz, H. F., Kelly, P. M. and Wigley, T. M. L., Northern hemisphere surface air temperature variations, 1851–1984. *J. Climate Appl. Meteorol.*, 1986, **25**, 161–179.
37. Lean, J., Skumanich, A. and White, O., Estimating the sun's radiative output during the Maunder minimum. *Geophys. Res. Lett.*, 1992, **19**, 1591–1594.
38. Lean, J., Beer, J. and Bradley, R., Reconstruction of solar irradiance since 1610: Implications for climatic change. *Geophys. Res. Lett.*, 1995, **22**, 3195–3198.
39. Lean, J., Living with a variable sun. *Physics Today*, 2005, 32–38.
40. Schneider, D., Living in sunny times. *Am. Sci.*, 2005, **93**, 22–24.
41. Haigh, J. D., The role of stratospheric ozone in modulating the solar radiative forcing of climate. *Nature*, 1994, **370**, 544–546.
42. Friis-Christensen, E. and Svensmark, H., What do we really know about the sun–climate connection? *Adv. Space Res.*, 1997, **20**, 913–921.
43. Rossow, W. B. and Cairns, B., Monitoring changes of clouds. *J. Climate*, 1995, **31**, 305–347.
44. Crowley, T. J., The geologic record of climate change. *Rev. Geophys. Space Phys.*, 1983, **21**, 828–877.
45. Markson, R. and Muir, M., Solar wind control on the earth's electric field. *Science*, 1980, **208**, 979–990.
46. Mehta, V. M. and Lau, K. M., Influence of solar irradiance on the Indian monsoon–ENSO relationship at decadal-multidecadal time scales. *Geophys. Res. Lett.*, 1997, **24**, 159–162.
47. Hiremath, K. M. and Mandi, P. I., Influence of the solar activity on the Indian monsoon rainfall. *New Astron.*, 2004, **9**, 651–662.
48. Bhattacharya, S. and Narasimha, R., Possible association between Indian monsoon rainfall and solar activity. *Geophys. Res. Lett.*, 2005, **32**, L05813.
49. Neff, U., Burns, S. J., Mudelsee, M., Mangini, A. and Matter, A., Strong coherence between solar variability and the monsoon in Oman between 9 and 6 kyrs ago. *Nature*, 2001, **411**, 290–293.
50. Fleitmann, D., Burns, S. J., Mudelsee, M., Neff, U., Kramers, J., Mangini, A. and Matter, A., Holocene forcing of the Indian monsoon recorded in a stalagmite from southern Oman. *Science*, 2003, **300**, 1737–1739.
51. Agnihotri, R., Dutta, K., Bhushan, R. and Somayajulu, B. L. K., Evidence for solar forcing on the Indian monsoon during the last millennium. *Earth Planet. Sci. Lett.*, 2002, **198**, 521–527.
52. Sarkar, A., Ramesh, R., Somayajulu, B. L. K., Agnihotri, R., Jull, A. J. T. and Burr, G. S., High resolution Holocene monsoon record from the eastern Arabian Sea. *Earth Planet. Sci. Lett.*, 2000, **177**, 209–218.
53. Wang, Y. *et al.*, The Holocene Asian monsoon: Links to solar changes and North Atlantic climate. *Science*, 2005, **308**, 854–857.
54. von Rad, U., Schaaf, M., Michels, K. H., Schulz, H., Berger, W. H. and Sirocko, F., A 5000-yr record of climate change in varved

sediments from the oxygen minimum zone off Pakistan, Northeastern Arabian Sea. *Quat. Res.*, 1999, **51**, 39–53.
55. Higginson, M. J., Altabet, M. A., Wincze, L., Herbert, T. D. and Murray, D. W., A solar (irradiance) trigger for millennial scale abrupt changes in the southwest monsoon? *Paleoceanography*, 2004, **19**, PA3015.
56. Staubwasser, M., Sirocko, F., Grootes, P. M. and Erlenkeuser, H., South Asian monsoon climate change and radiocarbon in the Arabian Sea during early and middle Holocene. *Paleoceanography*, 2002, **17**, 1063.
57. Ji, J., Shen, J., Balsam, W., Chen, J., Liu, L. and Liu, X., Asian monsoon oscillations in the northeastern Qinghai–Tibet Plateau since the late glacial as interpreted from visible reflectance of Qinghai Lake sediments. *Earth Planet. Sci. Lett.*, 2005, **233**, 61–70.
58. Castagnoli, G. C., Bonino, G., Caprioglio, F., Serio, M., Provenzale, A. and Bhandari, N., The $CaCO_3$ profile in a recent Ionian Sea core and the tree ring radiocarbon record over the last two millennia. *Geophys. Res. Lett.*, 1990, **17**, 1545–1548.
59. Hong, Y. T. *et al.*, Response of climate to solar forcing recorded in a 6000-year $\delta^{18}O$ time-series of Chinese peat cellulose. *The Holocene*, 2000, **10**, 1–7.
60. Hong, Y. T. *et al.*, A 6000-year record of changes in drought and precipitation in northeastern China based on a $\delta^{13}C$ time series from peat cellulose. *Earth Planet. Sci. Lett.*, 2001, **185**, 111–119.
61. Leuschner, D. C. and Sirocko, F., Orbital insolation forcing of the Indian Monsoon – A motor for global climate change. *Paleogeogr. Paleoclimatol. Paleoecol.*, 2003, **197**, 83–95.
62. Tiwari, M., Ramesh, R., Somayajulu, B. L. K., Jull, A. J. T. and Burr, G. S., Solar Control of Southwest Monsoon (SWM) on Centennial Time Scales. *Curr. Sci.*, 2005, **89**, 1583–1588.
63. Gupta, A. K., Das, M. and Anderson, D. M., Solar influence on the Indian summer monsoon during the Holocene. *Geophys. Res. Lett.*, 2005, **32**, L17703.
64. Wrytki, K., *Oceanographic Atlas of the International Indian Ocean Expedition*, National Science Foundation Publication, Washington DC, 1971, p. 531.
65. Ramesh, R. and Tiwari, M., Significance of stable oxygen ($\delta^{18}O$) and carbon ($\delta^{13}C$) isotopic compositions of individual foraminifera (*O. universa*) in a sediment core from the eastern Arabian Sea. In *Micropaleontology: Application in Stratigraphy and Paleoceanography* (ed. Sinha, D. K.), Narosa, New Delhi, 2005, pp. 331–350.
66. Bè, A. W. H., An ecological, zoogeographic and taxonomic review of recent planktonic foraminifera. In *Oceanic Micropaleontology* (ed. Ramsey, A. T. S.), Academic Press, London, 1977, pp. 1–100.
67. Fairbanks, R. G., Wiebe, P. H. and Bè, A. W. H., Vertical distribution and isotopic composition of living planktonic foraminifera in the western North Atlantic. *Science*, 1980, **207**, 61–63.
68. Shackleton, N. J., Oxygen isotope analyses and Pleistocene temperatures reassessed. *Nature*, 1967, **215**, 15–17.
69. Niitsuma, N., Oba, T. and Okada, M., Oxygen and carbon isotope stratigraphy at Site 723, Oman margin. *Proc. ODP Sci. Res.*, 1991, **117**, 321–341.
70. Fairbanks, R. G., A 17,000-year glacio-eustatic sea level record: Influence of glacial melting rates on the Younger Dryas event and deep ocean circulation. *Nature*, 1989, **342**, 637–642.
71. Rostek, F., Ruhland, G., Bassinot, F. C., Muller, P. J., Labeyrie, L. D., Lancelot, Y. and Bard, E., Reconstructing sea surface temperature and salinity using $\delta^{18}O$ and alkenone records. *Nature*, 1993, **364**, 319–321.
72. Guptha, M. V. S., Curry, W. B., Ittekkot, V. and Murlinath, A. S., Seasonal variation in the flux of Planktic foraminifera: Sediment trap results from the Bay of Bengal, Northern Indian Ocean. *J. Foraminiferal Res.*, 1997, **27**, 5–19.
73. McCreary, J. P., Kundu, P. K. and Molinari, R. L., A numerical investigation of dynamics, thermodynamics and mixed layer processes in the Indian Ocean. *Prog. Oceanogr.*, 1993, **31**, 181–224.
74. Shankar, D. and Shetye, S. R., On the dynamics of the Lakshdweep high and low in the southeastern Arabian Sea. *J. Geophys. Res.*, 1997, **102**, 12551–12562.
75. Thamban, M., Rao, V. P., Schneider, R. R. and Grootes, P. M., Glacial to Holocene fluctuations in hydrography and productivity along the southwestern continental margin of India. *Palaeogeogr. Palaeoclimatol. Palaeoecol.*, 2001, **165**, 113–127.
76. Duplessy, J. C., Bè, A. W. H. and Blanc, P. L., Oxygen and carbon isotopic composition of planktonic foraminifera in the Indian Ocean. *Palaeogeogr. Palaeoclimatol. Palaeoecol.*, 1981, **33**, 9–46.
77. Bard, E., Raisbeck, G., Yiou, F. and Jouzel, J., Solar irradiance during the last 1200 years based on cosmogenic nuclides. *Tellus B*, 2000, **52**, 985–992.
78. Schulz, M. and Mudelsee, M., Estimating red-noise spectra directly from unevenly spaced paleoclimatic time series. *Comput. Geosci.*, 2002, **28**, 421–426.
79. Usoskin, I. G. and Mursula, K., Long-term solar cycle evolution: Review of recent developments. *Sol. Phys.*, 2003, **218**, 319–343.
80. Lean, J. and Rind, D., Evaluating sun-climate relationships since the Little Ice Age. *J. Atmos. Sol. Terr. Phys.*, 1999, **61**, 25–36.

ACKNOWLEDGEMENTS. We thank ISRO–GBP for continued financial support for palaeoclimate studies and an anonymous referee for critical comments.

Received 10 May 2006; revised accepted 27 April 2007